

**Model-based extraction of material properties in multifrequency atomic force microscopy**Daniel Forchheimer,<sup>1</sup> Daniel Platz,<sup>1</sup> Erik A. Tholén,<sup>2</sup> and David B. Haviland<sup>1</sup><sup>1</sup>Royal Institute of Technology, Stockholm, Sweden<sup>2</sup>Intermodulation Products AB, Solna, Sweden

(Received 5 April 2012; revised manuscript received 27 April 2012; published 24 May 2012)

We present a method to reconstruct the nonlinear tip-surface force and extract material properties from a multifrequency atomic force microscopy (AFM) measurement with a high-quality-factor cantilever resonance. In a measurement time of  $\sim 2$  ms, we are able to accurately reconstruct the tip-surface force-displacement curve, allowing simultaneous high-resolution imaging of both topography and material properties at typical AFM scan rates. We verify the method using numerical simulations, apply it to experimental data, and use it to image mechanical properties of a polymer blend. We further discuss the limitations of the method and identify suitable operating conditions for AFM experiments.

DOI: [10.1103/PhysRevB.85.195449](https://doi.org/10.1103/PhysRevB.85.195449)

PACS number(s): 68.37.Ps, 07.79.-v, 62.25.-g, 05.45.-a

**I. INTRODUCTION**

Since its invention in the 1980s, the atomic force microscope has become an invaluable tool to image surfaces at the microscale and nanoscale levels. The need to image ever more complex structures has pushed development beyond the measurement of only topography, toward mapping quantitative material properties while scanning. Such imaging modes provide new means of investigating heterogeneous samples such as polymer blends or biological materials.

Previous studies have demonstrated quantitative atomic force microscopy (AFM) based on methods where the cantilever is driven at a single frequency while the motion response is measured at many harmonics.<sup>1-4</sup> In these experiments, the tip-surface force can be directly reconstructed from the tip motion and knowledge of the cantilever transfer function.<sup>1</sup> To obtain a rapidly changing tip-surface force, this direct method requires measuring the motion over a very broad frequency band to capture many harmonics of the drive frequency. These harmonic methods do not exploit the enhanced force sensitivity of a high-quality-factor cantilever resonance. Other methods excite the cantilever at multiple frequencies,<sup>5</sup> such as the resonance frequencies of several eigenmodes,<sup>6-8</sup> or multiple tones around one eigenmode.<sup>9,10</sup> While these methods work close to resonance and can thus expect a high sensitivity, the measurements typically contain too little information to be able to reconstruct a realistic tip-surface interaction.

We have previously demonstrated intermodulation AFM (ImAFM),<sup>11-14</sup> a multifrequency drive scheme which makes use of frequency mixing to transpose the information contained in the higher harmonics of a single drive tone to a narrow frequency band near resonance where the signal-to-noise ratio is high. The cantilever is driven with two tones at frequencies close to resonance, while the responding motion is measured at many mixing, or intermodulation, frequencies. Here we present a method of analysis to accurately reconstruct tip-surface forces from intermodulation spectra. In comparison to the direct force-reconstruction method from the broad band response, force reconstruction from this narrow band requires one additional assumption: a parametrized tip-surface force model. Our analysis shows that the intermodulation spectrum near resonance contains the information necessary to reconstruct a realistic tip-surface force and extract physical

model parameters. Through the reconstruction, we recover high-frequency components of the force which were buried below the measurement noise floor. The method is extremely general in that it allows for an *arbitrary* force model. We believe that the method can be applicable to many other multifrequency AFM modes and could find applications in the analysis of resonant nonlinear systems beyond AFM.

**II. EXTRACTING FORCE PARAMETERS FROM MOTION SPECTRA**

Force reconstruction aims at finding the nonlinear force acting between the surface and a small tip located at the end of an AFM cantilever, from a measurement of the tip motion,  $z(t)$ . As is common in the literature,<sup>15</sup> we model the cantilever as a point mass acted on by a linear cantilever restoring force, an external time-dependent drive force, and a nonlinear tip-surface force,

$$\frac{1}{\omega_0^2} \ddot{z}(t) + \frac{1}{Q\omega_0} \dot{z}(t) + z(t) = \frac{1}{k_c} f^{(\text{drive})}(t) + \frac{1}{k_c} f^{(\text{ts})}(z, \dot{z}), \quad (1)$$

where  $\omega_0$  is the resonance frequency of the first bending mode of the cantilever,  $k_c$  is its corresponding stiffness, and  $Q$  is its quality factor. Each of these constants and the constant converting output voltage of the optical detector to cantilever deflection can be calibrated by measuring the thermal noise force.<sup>16</sup>

By Fourier transforming Eq. (1), we arrive at an expression for the frequency dependence of the nonlinear tip-surface force,

$$\hat{f}^{(\text{ts})}(\omega) = k_c \hat{G}^{-1} [\hat{z}(\omega) - \hat{z}^{(\text{free})}(\omega)], \quad (2)$$

where  $\hat{G} = [(i\omega/\omega_0)^2 + i\omega/Q\omega_0 + 1]^{-1}$  is the linear transfer function of the harmonic oscillator, and  $\hat{z}^{(\text{free})}$  is the motion of the driven cantilever in the absence of the tip-surface force.

In ImAFM the cantilever is driven simultaneously with two tones at frequencies centered around the resonance and separated by  $\Delta\omega$ . If the drive frequencies are integer multiples of  $\Delta\omega$ , then the tip motion has a discrete spectrum with response only at frequencies that are also integer multiples of  $\Delta\omega$ . The signal can then be optimally sampled in the measurement time,

$T = 2\pi/\Delta\omega$ .<sup>11,17</sup> At frequencies far from a high-quality resonance, relatively large tip-surface forces give rise to very small tip motion, which typically cannot be detected above the noise floor. The measurable motion of the cantilever will therefore be limited to a narrow band,  $\Omega$ , close to resonance, where  $|G| \gg 1$ . In this frequency band, the cantilever is well described by a single eigenmode and the model given by Eq. (1) is a good approximation to the actual cantilever dynamics. We define a partial motion spectrum containing intermodulation response in the frequency band  $\Omega$ ,

$$\hat{Z}(\omega) = \begin{cases} \hat{z}(\omega) & \text{for } \omega \in \Omega, \\ 0 & \text{elsewhere.} \end{cases} \quad (3)$$

Taking the inverse Fourier transform of this partial spectrum, we arrive at a very good approximation to the real motion,

$$Z(t) = \mathcal{F}_\omega^{-1}[\hat{Z}(\omega)] \simeq z(t) \quad (4)$$

and the tip velocity

$$\dot{Z}(t) = \mathcal{F}_\omega^{-1}[i\omega\hat{Z}(\omega)] \simeq \dot{z}(t). \quad (5)$$

It should be stressed that while tip motion is limited to the band  $\Omega$ , the tip-surface force is not. The force spectrum contains strong components at frequencies many times the resonance frequency of the cantilever. The cantilever is, however, unable to sense these force components, and the challenge is to reconstruct the full force using only the partial motion spectrum.

Assuming that the force is described by a model function of the motion  $z(t)$ , the velocity  $\dot{z}(t)$ , and a set of parameters  $\mathbf{p}$ , our challenge is reduced to finding the parameter values which minimize the difference between the measured force and the force calculated from the model function at the frequencies in  $\Omega$ ,

$$k_c \hat{G}^{-1}(\hat{Z} - \hat{Z}^{(\text{free})}) - \mathcal{F}_t[f^{(\text{model})}(Z, \dot{Z}; \mathbf{p})] = \hat{\epsilon}(\omega; \mathbf{p}). \quad (6)$$

We can define an error function by summing the deviations  $\hat{\epsilon}(\omega)$  and minimize with respect to  $\mathbf{p}$ ,

$$E_{\min} = \min_{\mathbf{p}} \sum_{\omega \in \Omega} \text{Re}[\hat{\epsilon}(\omega; \mathbf{p})]^2 + \text{Im}[\hat{\epsilon}(\omega; \mathbf{p})]^2. \quad (7)$$

By minimizing  $E$ , we extract the optimal parameter values  $\mathbf{p}_{\text{opt}}$  and thereby reconstruct the model force  $f^{(\text{model})}(z, \dot{z}; \mathbf{p}_{\text{opt}})$  which best explains the measured motion. By summing the error only over intermodulation frequencies in the band  $\Omega$  where there is good signal-to-noise ratio, the spectrum of the reconstructed force outside the band  $\Omega$  is allowed to deviate substantially from that obtained directly from the measured data. Thus we see the tremendous advantage of performing the minimization in the frequency domain. In the time domain, it would be most difficult to separate the signal from the noise.

A numerical solver can be used for the minimization. Numerical algorithms require a reasonable initial estimate of the parameter values in order to converge to the global minimum. For the special case when the model is linear in all parameters, a unique solution can be found by matrix inversion, which is guaranteed to be the global minimum.<sup>13,14</sup>

### III. FORCE MODELS

The strength of the parameter extraction algorithm is that it can be applied to an arbitrary force model. We are especially interested in models motivated from contact mechanics such that the parameters have direct physical interpretation. The most common model used in AFM is the Derjaguin-Muller-Toropov (DMT) model for a spherical tip and a flat surface,

$$f^{(\text{ts})}(z) = \begin{cases} -F_{\text{vdW}} \frac{a_0^2}{(a_0+z+h)^2} & \text{for } z > -h, \\ -F_{\text{vdW}} + \frac{4}{3}R_{\text{DMT}}(-z-h)^{3/2} & \text{for } z \leq -h, \end{cases} \quad (8)$$

where  $h$  is the height of the equilibrium position of the tip above the surface.

We use a slightly different parametrization of the DMT model from that which is common in the literature<sup>15</sup> to aid the numerical solver. The parameter  $F_{\text{vdW}} = HR/6a_0^2$  is the maximum adhesion force due to van der Waals attraction, where  $H$  is the Hamaker constant,  $R$  is the tip radius, and  $a_0$  is the interatomic distance. For the contact regime, we introduce the DMT repulsion factor  $R_{\text{DMT}} = E^*\sqrt{R}$ , where  $E^*$  is the reduced Young's modulus. It is clear from the equations that it is not possible to unambiguously separate the material properties  $E^*$  and  $H$  from the tip radius  $R$  by measurement of the DMT force curve only. To do so would require a separate calibration of at least one of these three quantities, e.g., by blind tip reconstruction<sup>18</sup> or by measuring force on a reference surface.

Because the height  $h$  is a parameter of the force model, we can use the fitting procedure described above to determine  $h$  from the intermodulation spectrum. No independent measurement of  $h$  is required to generate the force-distance curve. During the time needed to measure one force curve (2 ms),  $h$  is assumed to be constant, and we can directly measure the minimum and maximum deflection of the cantilever,  $z_{\min}$  and  $z_{\max}$ . We can then define the peak penetration depth into the surface,

$$z_{\text{pen}} = z_{\min} - h, \quad (9)$$

as an alternative to the parameter  $h$ .

The DMT model is a conservative force model, but in real experiments there are also tip-surface interactions which dissipate energy. Investigation of such dissipative interactions is an ongoing field of research in AFM.<sup>19–21</sup> One class of dissipative force models are viscoelastic interactions in which the force not only depends on tip position but also linearly on tip velocity. The Voigt model is one such model, describing a distance-dependent viscous damping force when penetrating into the surface.<sup>22</sup> This dissipative force can be added to the conservative force,

$$f^{(\text{ts})}(z, \dot{z}) = \begin{cases} f^{(\text{cons})} & \text{for } z > -h, \\ f^{(\text{cons})} - \dot{z}D_V\sqrt{-(z+h)} & \text{for } z \leq -h. \end{cases} \quad (10)$$

The damping parameter  $D_V = \eta\sqrt{R}$ , where  $\eta$  is the viscosity of the material. The minimization procedure is used to extract  $D_V$  simultaneously with the conservative parameters. The validity of the Voigt model is not as well established in the AFM literature as the DMT model. Here we choose to use it to demonstrate the possibility to extract parameters

of nonconservative force models. We have observed that the extraction of parameters of the conservative DMT model is completely independent of the parameter of the dissipative Voigt model. In principle, not only viscoelastic parameters but parameters of essentially any force model, including complex dissipative forces which depend on the history of the tip motion, e.g., capillary force,<sup>23</sup> can be extracted using the described method.

#### IV. RESULTS AND DISCUSSION

We performed an ImAFM measurement on a poly(methyl methacrylate) (PMMA) thin film. The tip motion was sampled and a full motion spectrum was calculated and converted to a force spectrum using Eq. (2). A force spectrum at one probe height  $h$  is plotted with the blue curves in Fig. 1. The figure compares the intermodulation products around resonance  $f_0$  and around  $2f_0$ . Only a few signals are measurable above the noise near  $2f_0$ , where the noise-equivalent-force is greatly increased due to the reduced force sensitivity of the cantilever. Many more intermodulation products can be resolved near  $f_0$  in the frequency band  $\Omega$  with signal-to-noise ratio  $> 1$ . Using the measured partial spectrum in this band, we apply the force parameter extraction algorithm with the Voigt-DMT model (green dots in Fig. 1) to the measured force spectrum (blue curves in Fig. 1) in the band  $\Omega$ . The algorithm also reconstructs

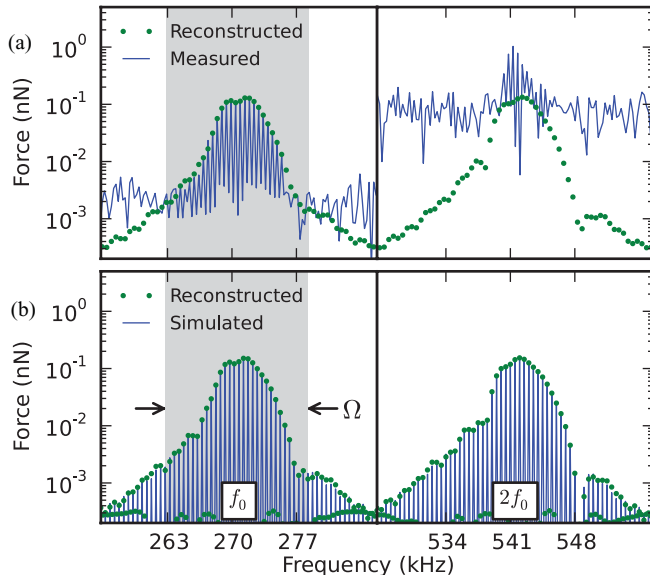


FIG. 1. (Color online) Spectrum of the tip-surface force in intermodulation AFM. The force can be reconstructed from the partial spectrum of intermodulation products contained in the band  $\Omega$  near resonance. (a) Experimental data acquired on poly(methyl methacrylate) with two drives,  $f_1 = 270.4$  and  $f_2 = 270.9$  kHz, producing a maximum free oscillation amplitude of 60 nm peak to peak. The amplitude at  $f_1$  in the measurement was 85% of its free amplitude. The cantilever had  $f_0 = 270.8$  kHz and  $Q = 416$ , and noise calibration gave  $k_c = 21$  N/m. Many peaks of the intermodulation spectrum near  $f_0$  are resolved above the noise. Intermodulation peaks near  $2f_0$  are buried in the detector noise. (b) Simulated force spectrum using the DMT-Voigt model and parameters extracted from the experimental data. The partial spectrum in the band  $\Omega$  contains enough information to reconstruct the full force spectrum.

TABLE I. Parameter values used in the simulation and corresponding parameters extracted from the partial motion spectrum in Fig. 1(b). The simulated parameters are equal to those extracted in Fig. 1(a) if the tip radius is assumed to be 10 nm.

	$h$ (nm)	$a_0$ (nm)	$F_{vdw}$ (nN)	$E^*$ (GPa)	$\eta$ (Pa s)
Simulated	23.00	1.60	1.56	1.00	71.00
Fitted	22.98	1.58	1.57	0.98	71.02

the force spectrum outside this band, where a lack of detector sensitivity prohibits force measurement.

A comparison around  $2f_0$  shows that the measured force amplitude is larger than the reconstructed force amplitude at the few frequencies where there is a measurable signal. This

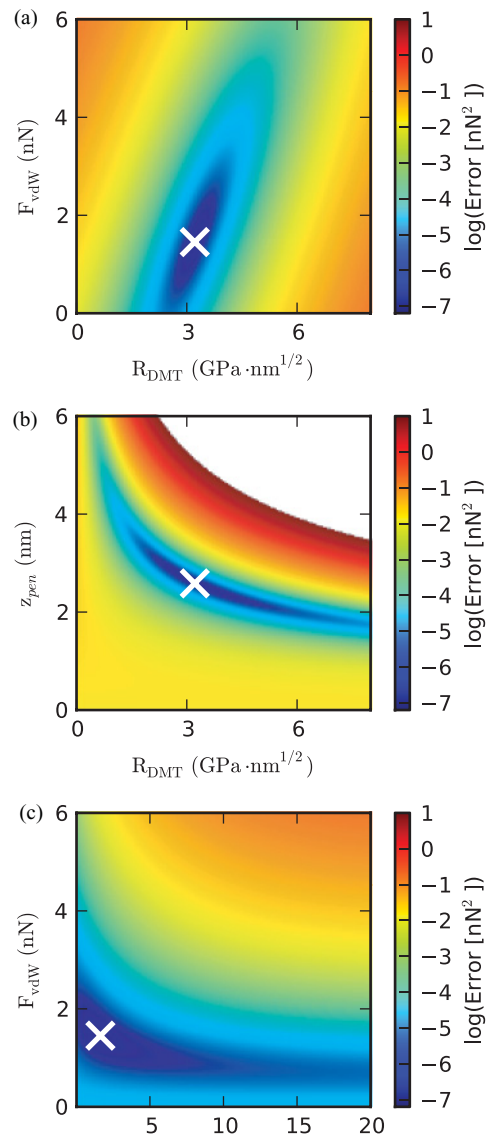


FIG. 2. (Color online) Two-dimensional cuts of the multidimensional error space. The magnitude of the error function  $E$  for the DMT-Voigt model is plotted in color against a few different pairs of parameters in the vicinity of the minimum. The white cross indicates the solution found by the numerical solver. The white area in (b) indicates that the error is larger than the range covered in the color bar.

is not surprising since the reconstruction does not take into account the higher eigenmodes of the cantilever and it therefore underestimates  $\hat{G}(\omega)$  at high frequencies. A better estimate of the cantilevers true transfer function would require calibration of several higher eigenmodes, a task which is not trivial and still the subject of research.<sup>24,25</sup> Luckily, this calibration is not needed if the tip motion is concentrated in the band  $\Omega$ .

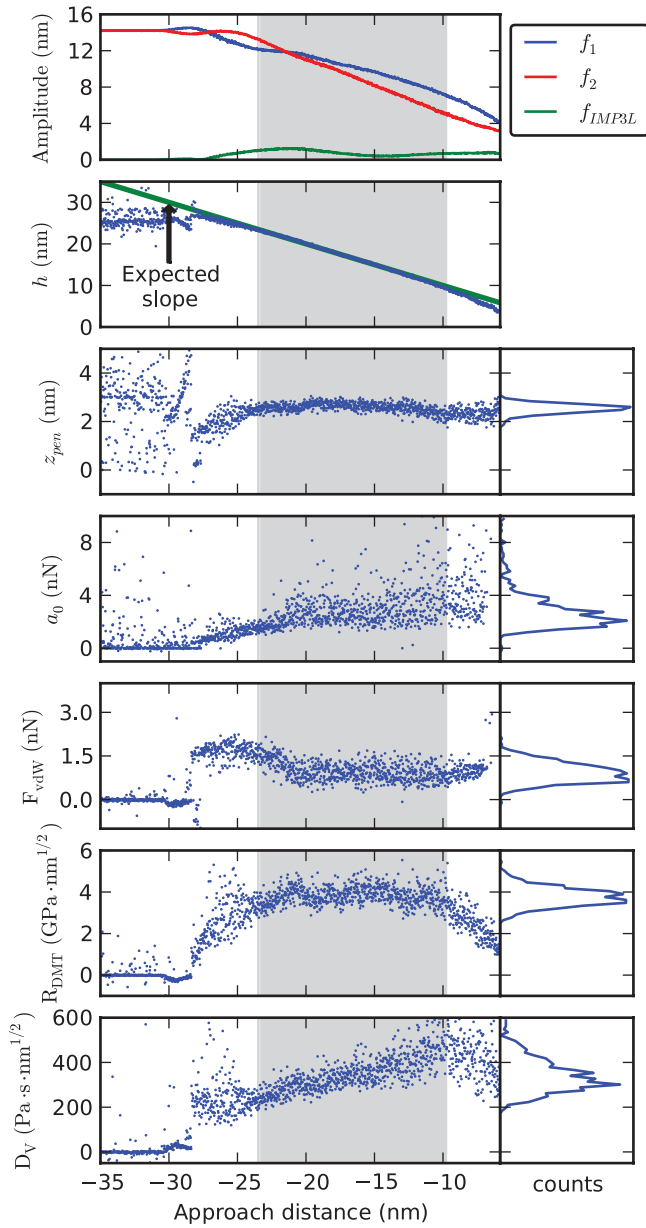


FIG. 3. (Color online) Dependence of the extracted parameter values on approach distance. Extraction of the DMT-Voigt parameters is performed for a slow approach to a PMMA surface with maximum free oscillation amplitude of 60 nm peak to peak. Further away than 30 nm the tip is not interacting with the surface and no parameters can be extracted. In a shaded region between roughly 25 and 10 nm away from the surface, the DMT repulsion  $R_{DMT}$  and adhesion  $F_{vdW}$  are constant, indicating a suitable working distance for extraction based on the DMT model. The observed change of the surface damping parameter  $D_V$  suggests that the Voigt damping has limited validity.

To further confirm the algorithm, we simulated the tip motion by numerical integration of Eq. (1) using the DMT-Voigt tip-surface force model with the parameters obtained from force reconstruction on the experimental data [see Fig. 1(b)]. The extraction algorithm was found to converge to correct model parameters (see Table I). The fact that we are able to recover the input parameters of the simulated motion from analysis of only the partial spectrum in the frequency band  $\Omega$  confirms that this spectrum does indeed contain enough information to fully determine the force. Furthermore, we see a remarkable similarity between the simulated and experimental force, and between the simulated and reconstructed force, both near  $f_0$  and near  $2f_0$ . Taken together, these observations demonstrate the ability of the intermodulation spectral method to predict signals that are buried below the noise floor in a measurement.

When performing nonlinear numerical optimization to find the model parameters, it is of importance to understand how the error  $E$  depends on the different parameters. The shape of the error in the parameter space communicates the sensitivity of the fit to changes in the parameters. For instance, it could be problematic for the solver if the error function has several local

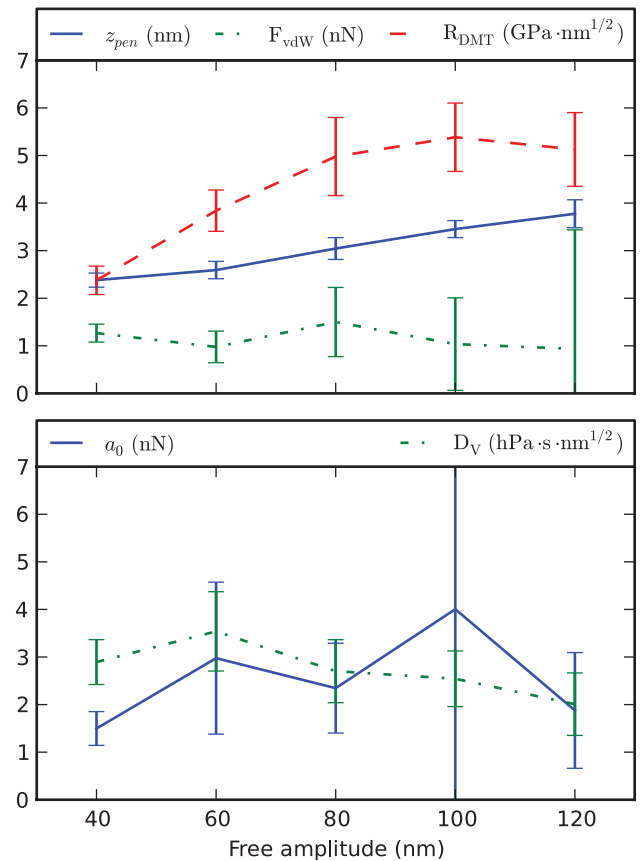


FIG. 4. (Color online) Dependence of the extracted parameter values on the drive amplitude. The drive amplitude is reflected in the measured maximum free oscillation amplitude. Parameters were extracted upon approach as in Fig. 3, and the mean value is plotted vs the free amplitude, where the error bars correspond to the standard deviation of the parameter values obtained in an interval where the amplitude at  $f_1$  was between 85% and 50% of its free value.

minima. The DMT-Voigt model has five free parameters so it is not possible to visualize the error in the entire parameter space with a two-dimensional (2D) plot. However, we can make 2D cuts by first finding the optimal values of all parameters and then plotting the error as a function of any two parameters, keeping the others constant. Figure 2 shows a few typical cuts generated from the experimental data of Fig. 1(a). The white crosses indicate the solution found by the solver and agree well with the global minimum in each cut.

From Fig. 2(a), we see that  $F_{vdW}$  vs  $R_{DMT}$  has an elliptical error space with one clear minimum. Thus we can expect it to be easy for the solver to converge for these parameters. In contrast, the error space of  $z_{pen}$  with respect to, for example,  $R_{DMT}$  contains regions of very high slope as well as very flat regions. We have noticed that the numerical optimization is sensitive to the initial value of  $z_{pen}$ , which must be within a few nm of the minimum for the solver to find a small error solution. An accurate initial guess of this parameter could be achieved using the polynomial reconstruction method previously described.<sup>13,14</sup> Empirically we find that the penetration depth  $z_{pen}$  varies less than the height  $h$  when scanning over the surface using the amplitude at the lower drive frequency as the feedback signal. It is therefore preferable to use  $z_{pen}$  rather than  $h$  in the parametrization of the force, as this makes it easier to guess an initial value. This observed variation in the extracted value of  $h$  demonstrates

that the feedback signal (so-called height signal in AFM) does not represent the true surface topography.

The parameter with the weakest influence on the error is  $a_0$ , which is plotted against  $F_{vdW}$  in Fig. 2(c). From the physical interpretation of the model,  $a_0$  is the interatomic distance and it is expected to be around 0.3 nm. However, in our measurements, we get a low error for values of  $a_0$  up to several tens of nm. We interpret this discrepancy as the presence of additional forces, in which case  $a_0$  represents the characteristic range of an effective, conservative attractive force.

Thus far we have discussed force reconstruction at a fixed height  $h$ . If the model used in reconstruction accurately describes the real tip-surface force, then one would expect the material parameters to be constant as  $h$  is varied. To test this, we measured the intermodulation spectrum while performing a slow and uniform approach of the cantilever base toward the PMMA film. This measurement allowed us to extract model parameters as a function of approach distance (see Fig. 3). We can identify a region where the adhesion force  $F_{vdW}$ , the DMT repulsion  $R_{DMT}$ , and  $a_0$  are essentially constant. This region is the suitable working distance to perform quantitative ImAFM measurements. While imaging, a feedback loop is adjusting the height of the cantilever above the surface to keep the response amplitude at the frequency  $f_1$  at a set value, somewhat lower than the free-response amplitude. A feedback amplitude set point in the range of 85% to 50% of the free amplitude is

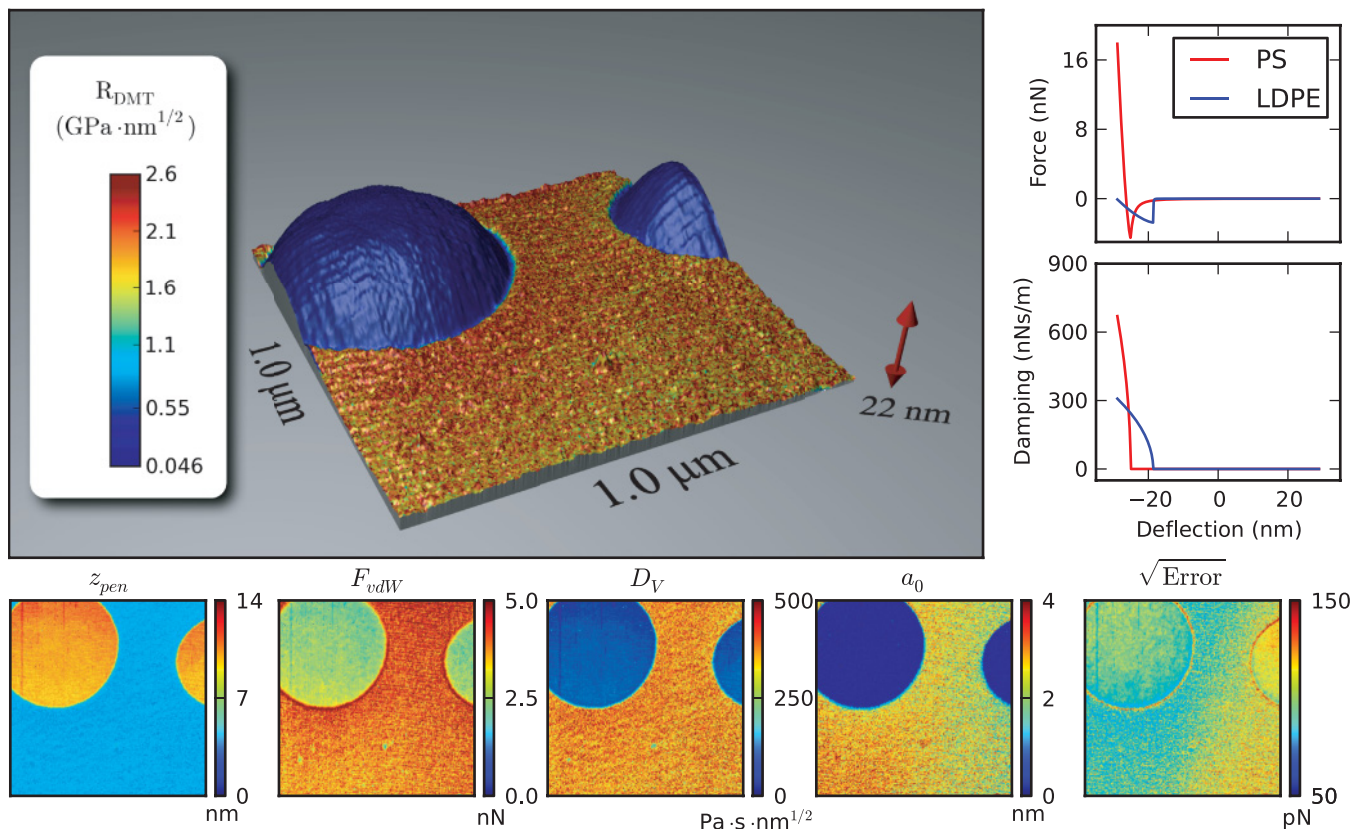


FIG. 5. (Color online) Surface parameter maps and representative force curves obtained from one ImAFM scan. Soft droplets of LDPE are revealed in a much stiffer PS matrix. A 3D rendering of the surface topography is color coded to give the DMT repulsion factor  $R_{DMT} = E^* \sqrt{R}$ , which is a tip-radius-dependent measure of the surface stiffness. 2D maps of the other parameters are shown together with a map of the fit error. Representative DMT force curves and Voigt damping curves are extracted and plotted for one point on the LDPE (blue curves) and one point on the PS (red curves).

found to give a suitable working distance above the surface (gray highlight in Fig. 3).

Figure 3 shows that the probe height  $h$ , which is extracted from the reconstruction algorithm, follows a line of slope  $-1$  when plotted versus the approach distance. This behavior demonstrates that the extracted  $h$  is in agreement with that measured by the calibrated scanner. We also see that the tip penetration into the material,  $z_{\text{pen}}$ , is independent of approach distance. The parameter  $a_0$  shows significant scatter, which can be understood as being a result of the weak error dependence discussed above. The dissipative parameter  $D_V$ , obtained from the Voigt model, is found to vary significantly with approach distance, indicating that the Voigt model is not very good.

We also investigated the dependence of the fitted parameters on the drive amplitude. Several approach studies as in Fig. 3 were made with different drive amplitudes and the mean and standard deviation of each parameter were determined within the region of suitable working distance. These are plotted versus the amplitude of free oscillation in Fig. 4. The observed increase of  $z_{\text{pen}}$  with increasing free oscillation amplitude demonstrates how deeper penetration into the material is achieved by increasing the drive to attain more stored energy in the oscillating cantilever, rather than lowering the amplitude set point. The extracted value of the DMT repulsion factor  $R_{\text{DMT}}$  seems to stabilize at higher drive amplitude, indicating that a free amplitude above 80 nm is a suitable operation condition for probing DMT contact mechanics.

Parameter extraction can also be performed on whole images to generate nanomechanical surface-property maps of heterogeneous materials. To demonstrate this, we scanned a polymer blend of polystyrene (PS) and low-density polyolefin (LDPE), recording and storing the intermodulation spectrum in the band  $\Omega$  at each of the  $256 \times 256$  pixels in the image. The scan file of size 25 MB contains all of the information needed to extract the parameters of a chosen interaction model at each pixel. Figure 5 shows a color map of the DMT repulsion parameter  $R_{\text{DMT}}$ , projected onto a 3D rendering of the surface topography.

We can see a sharp contrast between the softer LDPE ( $R_{\text{DMT}} = 0.006 \text{ GPa nm}^{1/2}$ ) and the stiffer PS ( $R_{\text{DMT}} = 4.5 \text{ GPa nm}^{1/2}$ ). The scan was performed at 1 line per second, which is a typical scanning speed for single-frequency dynamic AFM, where this sample shows a high-quality phase image with sharp contrast. At this scan speed, ImAFM acquires some 20 amplitude and phase images with good contrast, which together enable a detailed study of the changes in material properties that are responsible for the observed contrast. Figure 5 also shows two representative force curves extracted at one point on the LDPE and PS, respectively, as well as smaller maps of the DMT-Voigt parameters extracted from the scan. The image of the square root of the error allows us to identify areas where the minimization was less successful at the interface between the two polymers.

## V. CONCLUSION

Intermodulation AFM has the ability to rapidly generate detailed quantitative maps of surface mechanical properties. The method exploits frequency mixing to greatly increase

the information available in the narrow band near resonance, where sensitivity of measurement is highest and where accurate calibration can be performed. Comparing experimental data and numerical simulation, we showed that this information is sufficient to fully reconstruct the tip-surface force. We verified the consistency of the method by showing that extracted parameters were constant in a suitable range of working distance. The method, which works with standard cantilevers and is easy to implement on any AFM, should find widespread use in many areas of material science where detailed quantitative images of surface mechanical properties are desired.

## ACKNOWLEDGMENTS

The authors acknowledge financial support from the Swedish Research Council (VR) and the Swedish Government Agency for Innovation Systems (VINNOVA).

## APPENDIX A: EXPERIMENTAL DETAILS

### 1. Sample preparations

The sample used in Figs. 1–4 was made by spin casting poly(methyl methacrylate) 4% in anisol on an oxidized silicon wafer for 1 min at 3000 rpm, resulting in a 250 nm thin film. The sample in Fig. 5 was a blend of polystyrene and low-density polyolefin elastomer (PS-LDPE) spin cast on a silicon (Bruker).

### 2. Atomic force microscopy measurements

All AFM measurements were done using a Dimension 3100 (Veeco) equipped with an intermodulation lock-in analyzer (ImLA)<sup>17</sup> and the ImAFM software suite, including the quantitative analysis package from Intermodulation Products AB (Stockholm, Sweden). The ImLA creates the drive signal to excite the AFM cantilever, analyzes the deflection signal, and creates the error signal used for feedback while scanning. The ImLA can be run in a streaming mode where it works as a synchronous digital waveform generator and digital acquisition card that optimally samples data and sends it to a computer for Fourier transform, or in lock-in mode where the ImLA calculates in parallel the spectral data at 32 predefined frequencies and sends the result to the computer for storage. The streaming mode was used in Figs. 1–4. In these figures, the AFM was set to perform approach curves, in which the base of the cantilever was moved at a constant speed of 100 nm/s towards the surface. Figure 5 was performed in imaging mode with the AFM feedback loop adjusting the  $z$ -piezo to keep the amplitude at  $f_1$  at 80% of its free amplitude; data was obtained from the ImLA using the lock-in mode.

The cantilevers used had a nominal resonance frequency of  $f_0 = 300 \text{ kHz}$  and stiffness of  $k_c = 40 \text{ N/m}$  (BudgetSensors, Bulgaria), although each cantilever was calibrated using the thermal noise calibration method before use. In Figs. 1–4, the calibration gave  $f_0 = 270.76 \text{ kHz}$ ,  $k_c = 21 \text{ N/m}$ , and a quality factor of  $Q = 416$ . The two drive frequencies were set at  $f_1 = 270.40$  and  $f_2 = 270.90 \text{ kHz}$ , giving a

beat frequency of  $\Delta f = 500$  Hz. Figure 5 was obtained in a separate experiment with  $f_0 = 315.47$  kHz,  $k_c = 32$  N/m,  $Q = 574$ ,  $f_1 = 315.21$  kHz, and  $f_2 = 315.71$  kHz. The measurement time for force reconstruction was exactly one beat,  $1/\Delta f = 2$  ms, except in Fig. 1 where twice that time was used in order to show the discreteness of the intermodulation spectrum. The drive amplitudes were adjusted until the response amplitude at both drive frequencies was equal and the desired maximum peak-to-peak amplitude was reached.

### 3. Numerics

Simulations were done using CVODE v2.6.0 (Ref. 26) to numerically integrate the equation of motion (1) with a DMT-Voigt model as the nonlinear tip-surface force. This nonlinear ordinary differential equation (ODE) solver has discrete event detection, which allowed us to properly treat the discontinuity in the force gradient at  $z = h$ . The minimization for parameter extraction, given by Eq. (6), was performed with the “optimize.leastsq” module in SCIPY v0.9.0, implementing the Levenberg-Marquardt algorithm.<sup>27</sup>

- 
- <sup>1</sup>M. Stark, R. W. Stark, W. M. Heckl, and R. Guckenberger, *Proc. Natl. Acad. Sci. USA* **99**, 8473 (2002).
- <sup>2</sup>J. Legleiter, M. Park, B. Cusick, and T. Kowalewski, *Proc. Natl. Acad. Sci. USA* **103**, 4813 (2006).
- <sup>3</sup>O. Sahin, S. Magonov, C. Su, C. F. Quate, and O. Solgaard, *Nature Nanotechnol.* **2**, 507 (2007).
- <sup>4</sup>A. Fatih Sarioglu, S. Magonov, and O. Solgaard, *Appl. Phys. Lett.* **100**, 053109 (2012).
- <sup>5</sup>R. García and E. T. Herruzo, *Nature Nanotechnol.* **7**, 217 (2012).
- <sup>6</sup>T. R. Rodríguez and R. García, *Appl. Phys. Lett.* **84**, 449 (2004).
- <sup>7</sup>S. D. Solares and G. Chawla, *J. Appl. Phys.* **108**, 054901 (2010).
- <sup>8</sup>R. Proksch, *Appl. Phys. Lett.* **89**, 113121 (2006).
- <sup>9</sup>S. Jesse, S. V. Kalinin, R. Proksch, a. P. Baddorf, and B. J. Rodriguez, *Nanotechnology* **18**, 435503 (2007).
- <sup>10</sup>B. J. Rodriguez, C. Callahan, S. V. Kalinin, and R. Proksch, *Nanotechnology* **18**, 475504 (2007).
- <sup>11</sup>D. Platz, E. A. Tholén, D. Pesen, and D. B. Haviland, *Appl. Phys. Lett.* **92**, 153106 (2008).
- <sup>12</sup>D. Platz, E. A. Tholén, C. Hutter, A. C. von Bieren, and D. B. Haviland, *Ultramicroscopy* **110**, 573 (2010).
- <sup>13</sup>C. Hutter, D. Platz, E. A. Tholén, T. H. Hansson, and D. B. Haviland, *Phys. Rev. Lett.* **104**, 050801 (2010).
- <sup>14</sup>D. Platz, D. Forchheimer, E. A. Tholén, and D. B. Haviland, [arXiv:1202.5217](https://arxiv.org/abs/1202.5217) [IOP Nanotechnol. (to be published)].
- <sup>15</sup>R. García, *Surf. Sci. Rep.* **47**, 197 (2002).
- <sup>16</sup>M. J. Higgins, R. Proksch, J. E. Sader, M. Polcik, S. Mc Endoo, J. P. Cleveland, and S. P. Jarvis, *Rev. Sci. Instrum.* **77**, 013701 (2006).
- <sup>17</sup>E. A. Tholén, D. Platz, D. Forchheimer, V. Schuler, M. O. Tholén, C. Hutter, and D. B. Haviland, *Rev. Sci. Instrum.* **82**, 026109 (2011).
- <sup>18</sup>L. Dongmo, J. Villarrubia, S. Jones, T. Renegar, M. Postek, and J. Song, *Ultramicroscopy* **85**, 141 (2000).
- <sup>19</sup>J. E. Sader, T. Uchihashi, M. J. Higgins, A. Farrell, Y. Nakayama, and S. P. Jarvis, *Nanotechnology* **16**, S94 (2005).
- <sup>20</sup>S. Hu and A. Raman, *Nanotechnology* **19**, 375704 (2008).
- <sup>21</sup>U. Dürig, *New J. Phys.* **2**, 5 (2000).
- <sup>22</sup>R. García, C. Gómez, N. Martínez, S. Patil, C. Dietz, and R. Magerle, *Phys. Rev. Lett.* **97**, 016103 (2006).
- <sup>23</sup>S. Santos, A. Verdaguer, T. Souier, N. H. Thomson, and M. Chiesa, *Nanotechnology* **22**, 465705 (2011).
- <sup>24</sup>D. Kiracofe and A. Raman, *J. Appl. Phys.* **107**, 033506 (2010).
- <sup>25</sup>J. R. Lozano, D. Kiracofe, J. Melcher, R. Garcia, and A. Raman, *Nanotechnology* **21**, 465502 (2010).
- <sup>26</sup>A. C. Hindmarsh, P. N. Brown, K. E. Grant, S. L. Lee, R. Serban, D. A. N. E. Shumaker, and C. S. Woodward, *ACM Trans. Math. Software* **31**, 363 (2005).
- <sup>27</sup>J. Moré, in *Numerical Analysis*, edited by G. Watson (Springer, Berlin/Heidelberg, 1978), Vol. 630, pp. 105–116.